Inorganic Chemistry

Article

pubs.acs.org/IC

Probing the Oxidation Chemistry of Half-Sandwich Iridium Complexes with Oxygen Atom Transfer Reagents

Christopher R. Turlington, Daniel P. Harrison,† Peter S. White, Maurice Brookhart, and Joseph L. Templeton*

W. R. Kenan Laboratory, Department of Chemistry, University of North Carolina at Chapel Hill, Chapel Hill, North Carolina 27599-3290, United States

Supporting Information

ABSTRACT: The new complexes [Ir(Cp*)(phpy)3,5-bis-(trifluoromethyl)benzonitrile]$^+$ (**1-NCAr$^+$**) and [Ir(Cp*)-(phpy)(styrene)]$^+$ (**1-Sty$^+$**, Cp* = η^5-pentamethylcyclopenta-dienyl, phpy = 2-phenylene-$\kappa C^{1'}$-pyridine-κN) were prepared as analogues of reported iridium water oxidation catalysts, to study their reactions with oxygen atom transfer (OAT) reagents at low temperatures. In no case was the desired product, an Ir(V)oxo complex, observed by spectroscopy. Instead, ligand oxidation was implicated. Oxidation of **1-NCAr$^+$** with the OAT reagent dimethyldioxirane (DMDO) yielded dioxygen when analyzed by GC, but formation of a heterogeneous or paramagnetic species was simultaneously observed. This amplifies uncertainty over the actual identity of iridium catalysts in the harsh oxidizing conditions required for water oxidation. Catalyst stability was then assessed for a reported styrene epoxidation mediated by [Ir(Cp*)(phpy)(OH$_2$)]$^+$ (**1-OH$_2^+$**). It was found that the OAT reagent iodosobenzene (PhIO) extensively oxidized the organic ligands of **1-OH$_2^+$**. Acetic acid was detected as a decomposition product. In addition, both the molecular structure and the aqueous electrochemistry of **1-OH$_2^+$** are described for the first time. Oxidative scans revealed rapid decomposition of the complex. All of the above experiments indicate that degradation of the organic ligands in catalysts built with the Ir(Cp*)(phpy) framework are facile under oxidizing conditions. In separate experiments designed to promote ligand substitution, an unexpected silver-bridged, dinuclear Ir(III) species with terminal hydrides, [{Ir(Cp*)(phpy)H}$_2$Ag]$^+$ (**2**), was discovered. The source of Ag$^+$ for complex **2** was identified as AgCl.

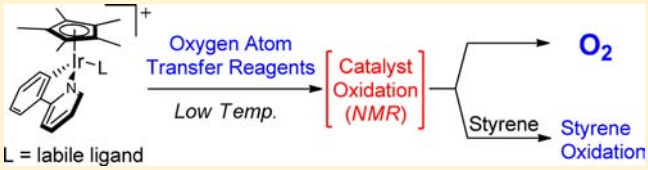

INTRODUCTION

Molecular iridium catalysts for water oxidation have received considerable attention.[1−7] These catalysts were originally considered to be homogeneous molecular catalysts when the oxidation was driven by ceric ammonium nitrate (CAN), and the reactive species was postulated to be an Ir(V)oxo species.[8,9] A popular ligand framework employs the η^5 Cp* ligand to form half-sandwich complexes, often in conjunction with a chelating κ^2 ligand. Many catalysts have been reported with this motif.[4−8]

Later work raised significant questions about catalyst stability.[10−12] Water oxidation experiments typically employ the harsh oxidant CAN in excess of 100−10,000 equivalents. To study catalyst evolution with fewer equivalents of oxidant, Grotjahn et al. acquired scanning transmission electron microscopy (STEM) images after 15 min of water oxidation with Ir(Cp*)(phpy)Cl (**3**) and 58 equiv of CAN (Scheme 1a).[13] The STEM images revealed significant agglomeration of iridium- and cerium-based particles. Although nanoparticle formation can occur during STEM sample preparation or from electron beam impact during data collection, many representative Ir(Cp*) catalysts required 15−30 equiv of CAN before oxygen evolution started.[13] A homogeneous process requires only 4 equiv of CAN to generate 1 equiv of oxygen, so modification of the ligands of the catalyst may occur before the onset of oxygen evolution.

Scheme 1. (a) Aqueous Oxidation of 3 with 58 equiv of CAN[a] and (b) CAN Oxidation of a Representative Ir(Cp*) Catalyst[b] (ref 13)

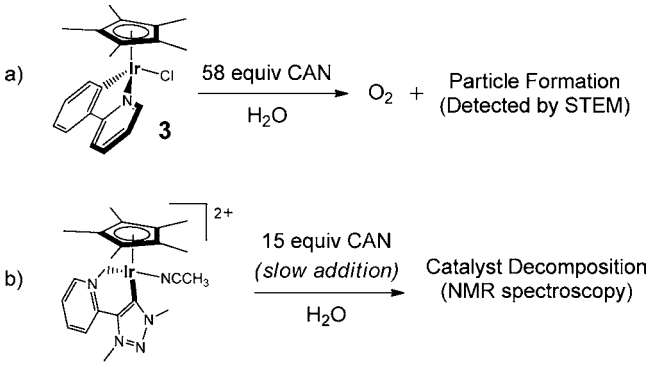

[a]Particles were detected in STEM images after 15 minutes.

[b]Monitored by NMR spectroscopy in D_2O. Complete degradation of the catalyst was observed.

Received: June 27, 2013
Published: September 24, 2013

Compelling evidence for ligand oxidation was obtained when the catalysts were slowly treated with 15 equiv of CAN in D_2O, and the reactions were monitored by NMR spectroscopy. Even addition of 1 equiv of CAN to a representative Ir(Cp*) catalyst (pictured in Scheme 1b) resulted in loss of 16% of the complex after 20 min. As 14 more equivalents of CAN were added over an additional 3 h, the characteristic signals of the metal complex disappeared completely, and were replaced by many signals of low intensity. Acetic and formic acids were identified at the end of the oxidative reaction sequence, and such oxidative degradation was witnessed for all of the catalysts tested.[13] Later NMR studies by Macchioni confirmed that Ir(Cp*) catalysts can evolve acetic, formic, and glycolic acids when oxidized with a large excess of CAN (>450 equiv).[14,15]

Evidence for homogeneous catalysis was obtained when using sodium periodate as the sacrificial oxidant in place of CAN. Crabtree and co-workers have employed time-resolved dynamic light scattering (DLS) as an effective method to probe for heterogeneous particles, and they have concluded that molecular iridium catalysts are responsible for water oxidation and C−H hydroxylation in the presence of excess sodium periodate (Scheme 2a).[16,17] New bidentate ligands that are

Scheme 2. (a) Homogeneous Iridium-Catalyzed Water Oxidation and Hydroxylation Reactions Driven by Sodium Periodate, and (b) Sacrificial Loss of the Cp* Ligand of 4 Is Required for Catalyst Activation

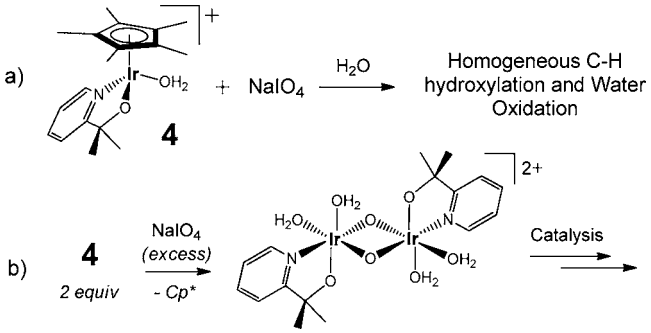

more stable under oxidative conditions, such as 2-(2′-pyridyl)-2-propanolate (pictured in Scheme 2), also help stabilize molecular catalysts. Even in systems using sodium periodate and robust bidentate ligands, however, initial oxidation of the complex results in sacrificial oxidation and displacement of the Cp* ligand. Experimental evidence suggested that the homogeneous resting state of precatalyst **4** was a dinuclear, Ir^{IV}(bis-μ-oxo)Ir^{IV} species (Scheme 2b).[18] Oxidation to Ir(V) could yield the active species.[18] These studies demonstrate that alteration of the ligand environment (sacrificial loss of the Cp* ligand) was still necessary to achieve homogeneous catalysis with sodium periodate.

Although recent work has revealed oxidative alteration or degradation of Ir(Cp*) complexes, we postulated that stoichiometric oxidations of Ir(Cp*)(phpy) complexes with oxygen atom transfer (OAT) reagents at low temperatures might allow spectroscopic detection of a high-valent Ir(V)oxo species (Scheme 3). Using OAT reagents offers the possibility of completing the two electron oxidation to a terminal oxo in one step, and switching from aqueous to organic solvents would allow reactions to be run at low temperatures. Low temperatures would improve the chance of observing oxidation products. Iridium complexes with terminal oxo ligands are rare;

Scheme 3. Strategy for Observing an Ir(V)oxo Complex at Low Temperatures in Organic Solvents

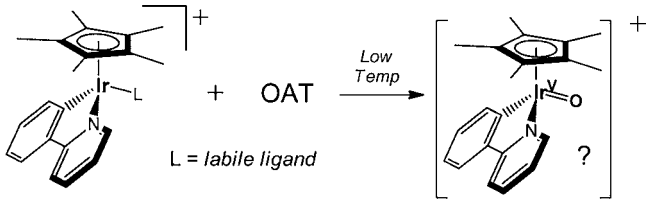

only two examples are known.[19,20] Terminal oxo ligands on late transition metals are uncommon since filled dπ orbitals on the metal and filled p orbitals on a terminal oxide engender destabilizing, repulsive four-electron interactions (Figure 1).[21]

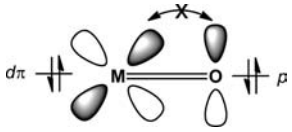

Figure 1. Repulsive interaction between filled dπ orbitals on metal and filled p orbitals that destabilize a late transition metal oxo complex.

Motivation for this work included literature precedence for platinum oxo formation. Milstein reported a Pt(IV)oxo complex through OAT to a Pt(II)pincer complex using dimethyldioxirane (DMDO).[22] An important feature of this experiment was the use of acetone as a highly labile ligand on the Pt(II) precursor, which allowed the OAT reagent to react at the metal center. Inspired by this report, we utilized analogous conditions for our attempts to oxidize iridium complexes that were models of water oxidation catalysts.

In addition, we desired to study the aqueous electrochemistry of **1-OH$_2^+$**, a proposed intermediate in a water oxidation reaction.[4] Two proton-coupled electron transfer (PCET) events would result in the net loss of two protons and two electrons, yielding a transient Ir(V)oxo species. PCET oxidations can often be observed electrochemically in aqueous solutions. For these reasons, it was believed that **1-OH$_2^+$** would be a viable complex to probe for evidence of a high-valent iridium species competent for water oxidation.

This work describes our attempts to observe an Ir(V)oxo species using derivatives of **3**, a reported water oxidation catalyst.[8,23] When stoichiometric oxidations did not yield an observable Ir(V)oxo species, reactions with excess oxidant were studied to investigate catalyst stability. It was found that **1-NCAr$^+$** reacted with multiple equivalents of DMDO, generating oxygen. This process, however, could not be definitively assigned to a homogeneous catalytic cycle. An epoxidation reaction with **1-OH$_2^+$**, styrene, and iodosobenzene (PhIO) was also monitored. The reaction generated acetic acid, a product of organic ligand degradation. The structure of **1-OH$_2^+$** is reported, but the complex is unstable when oxidized electrochemically. These experiments highlight the difficulties associated with observing homogeneous high-valent iridium species, and demonstrate that oxygen evolution or olefin oxidation is not easily assigned to such molecular species. Finally, an unexpected, silver-bridged dinuclear iridium species formed in the presence of AgCl and Ir(Cp*)(phpy)H.[24]

dx.doi.org/10.1021/ic4016405 | Inorg. Chem. 2013, 52, 11351−11360

RESULTS AND DISCUSSION

Synthesis of Iridium Complexes. A goal of this project was to synthesize an iridium complex with a weakly coordinating ligand to study OAT, analogous to Milstein's work.[22] Accordingly, we prepared [Ir(Cp*)(phpy)(3,5-bis(trifluoromethyl)benzonitrile)][$B(Ar^F)_4$] (**1-NCAr**$^+$, $B(Ar^F)_4$ = tetrakis[3,5-bis(trifluoromethyl)phenyl]borate). This was accomplished by halide abstraction from **3** with Na[$B(Ar^F)_4$] in the presence of the nitrile ligand, 3,5-bis(trifluoromethyl)-benzonitrile (Scheme 4). The reaction was complete within 1 h

Scheme 4. Synthesis of [Ir(Cp*)(phpy)L][$B(Ar^F)_4$] Complexes

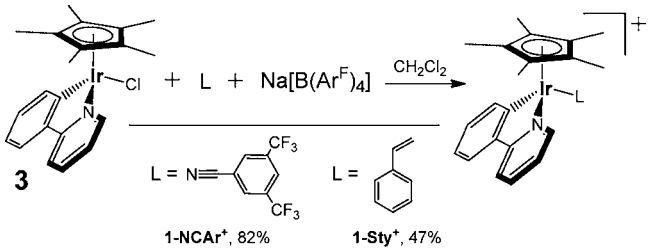

in dichloromethane at room temperature. Notably, the nearly overlapping resonances of the aromatic protons of the nitrile ligand shifted from 8.16 ppm (2H) and 8.15 (1H) in dichloromethane-d_2 to 8.15 ppm (1H) and 7.83 (2H) upon coordination to the metal. This allowed convenient distinction between bound or free nitrile in OAT reactions. Even though **1-NCAr**$^+$ has a weak two-electron nitrile donor ligand, the complex is neither water sensitive nor air sensitive and can be stored on the benchtop indefinitely.

A styrene derivative, [Ir(Cp*)(phpy)(styrene)][$B(Ar^F)_4$] (**1-Sty**$^+$), was prepared in an analogous manner to **1-NCAr**$^+$. Complex **1-Sty**$^+$ was studied in styrene epoxidation reactions, as styrene readily displaced weaker ligands from Ir(Cp*)(phpy) precatalysts to form **1-Sty**$^+$.

The complex [Ir(Cp*)(phpy)(OH_2)][OTf] (**1-OH_2**$^+$) was prepared according to a known procedure (OTf = trifluoromethanesulfonate).[25] Crystals suitable for X-ray diffraction studies were grown by layering pentane on top of a concentrated solution of **1-OH_2**$^+$ in dichloromethane, and the molecular structure is reported here for the first time (Figure 2).[26] The aqua protons were located during refinement of the structure, establishing that water is the sixth ligand in the coordination sphere. Each aqua proton was within hydrogen bonding distance to a triflate anion in the crystal lattice. The iridium–oxygen bond length is 2.176 Å, which is within the midrange for reported iridium aqua distances (2.136 Å–2.243 Å).[27,28] For comparison, the bipyridine (bpy) derivative, [Ir(Cp*)(bpy)(OH_2)]$^{2+}$, has an iridium oxygen bond length of 2.153 Å.[29] The bpy complex presumably has a shorter iridium–oxygen bond length because it is a dication. When a noncoordinating $^-B(Ar^F)_4$ anion was substituted for the $^-$OTf anion, it was found that [**1-OH_2**][$B(Ar^F)_4$] was stable in methanol and acetone, but it decomposed within 30 min to unidentified species in common organic solvents such as benzene, chloroform, and dichloromethane. Even when stored as a solid in a glovebox freezer at −25 °C, [**1-OH_2**][$B(Ar^F)_4$] decomposed over 5 months into intractable materials. The inherent instability of [**1-OH_2**][$B(Ar^F)_4$] was surprising.

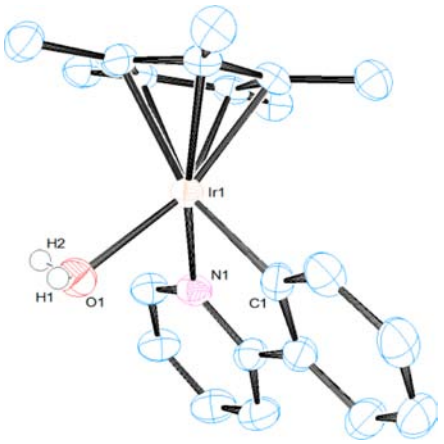

Figure 2. ORTEP drawing of **1-OH_2**$^+$, with partial numbering scheme. Ellipsoids are drawn at the 50% probability level. The anion and the hydrogen atoms on the Cp* and phpy moieties are omitted for clarity. Selected bond lengths (Å) and bond angles (deg): Ir_1–O_1 2.176(3), Ir_1–N_1 2.089(4), Ir_1–C_1 2.055(4), O_1–Ir_1–C_1 87.26(15), N_1–Ir_1–O_1 81.88(14), C_1–Ir_1–N_1 78.29(16).

Reaction of 1-NCAr$^+$ with Dimethyldioxirane (DMDO). In a reaction monitored by NMR spectroscopy in acetone-d_6, the reagent DMDO (added as a solution in acetone)[30] disappeared over 50 min at −50 °C in the presence of 1 equiv of cationic iridium complex **1-NCAr**$^+$. DMDO does not decompose at an appreciable rate in the absence of metal under these reaction conditions.[31] Less than 10% of the coordinated nitrile ligand was displaced (Supporting Information, Figure S5), but no other iridium species was detected over the course of the reaction. The reaction products, therefore, were either NMR silent or buried beneath the large acetone peak.

In the reaction with DMDO we postulated that **1-NCAr**$^+$ was the resting state for a homogeneous catalytic cycle that generates dioxygen from DMDO (Scheme 5). OAT from DMDO to **1-NCAr**$^+$ could generate a transient [Ir^V(Cp*)-

Scheme 5. Possible Catalytic Cycle for Homogeneous Oxygen Evolution from DMDO Catalyzed by 1-NCAr$^+$

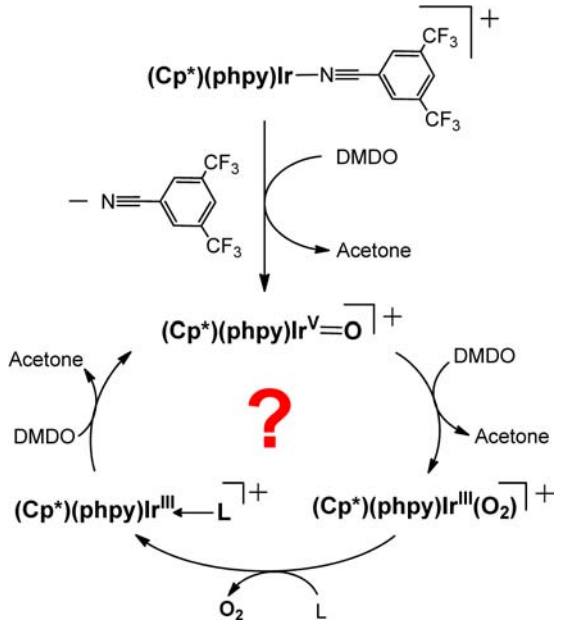

dx.doi.org/10.1021/ic4016405 | Inorg. Chem. 2013, 52, 11351–11360

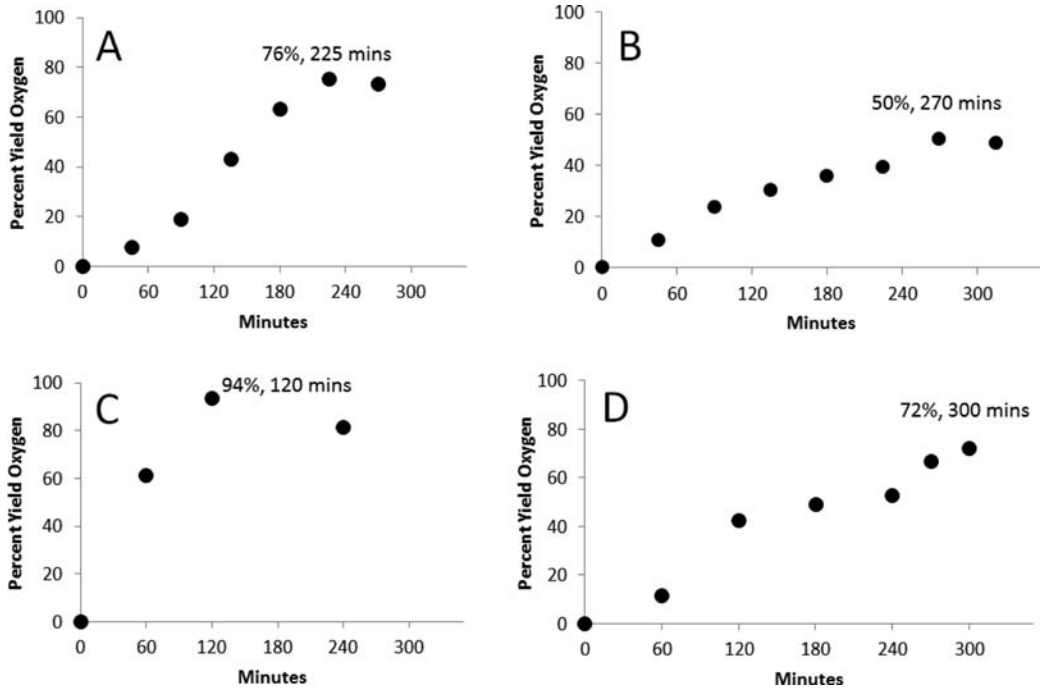

Figure 3. Oxygen evolution from DMDO catalyzed by **1-NCAr**$^+$ (17 mol %) at −40 °C. The overall percent yield of dioxygen (based on DMDO) was plotted as a function of time for reactions A−D, pictured above. Reactions C and D were run side-by-side. Irreproducible results suggested that a homogeneous mechanism was unlikely.

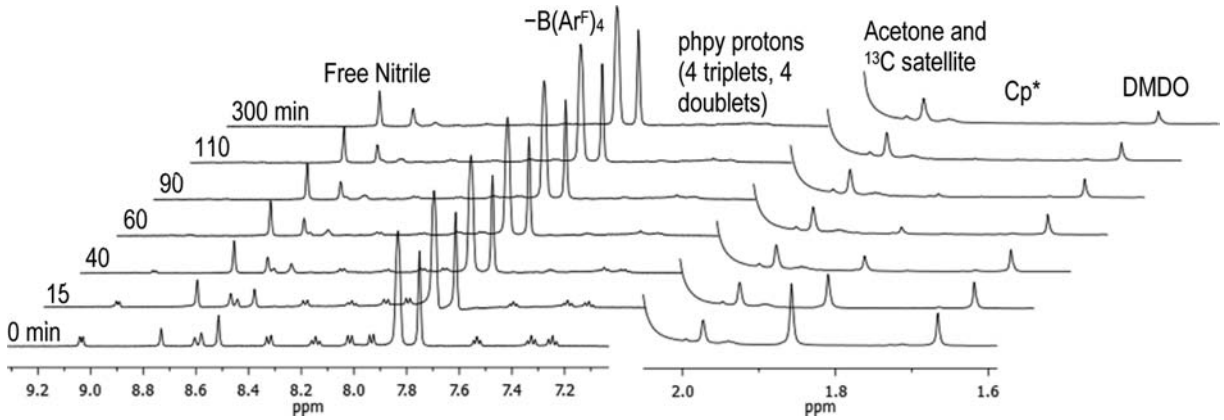

Figure 4. Time resolved NMR spectra of reaction of **1-NCAr**$^+$ and 6 equiv of DMDO at −40 °C. Complete disappearance of **1-NCAr**$^+$ was observed after 2 h, but no decomposition products were observed by NMR spectroscopy. A heterogeneous species or paramagnetic species was likely the product. DMDO continued to react over 5 h.

(phpy)O]$^+$ complex, analogous to Milstein's reported DMDO oxidation of a Pt(II)pincer to form a Pt(IV)oxo complex.[22] A terminal Ir(V)oxo species is expected to be electrophilic at oxygen, allowing for nucleophilic attack.[8] A lone pair of electrons on a DMDO oxygen atom could serve as a nucleophile, leading to oxygen−oxygen bond formation and a two-electron reduction of iridium. Loss of acetone would lead to a dioxygen complex, [Ir(Cp*)(phpy)O_2]$^+$, which could liberate dioxygen, completing the catalytic cycle. The products of such a catalytic cycle, oxygen and acetone, would be undetected in the ^{1}H NMR experiment. Acetone is already present in such a large excess (because it is the solvent for DMDO) that a small increase could not be reliably measured. Our initial hypothesis was to invoke a homogeneous Ir(III)/Ir(V) process to account for these results.

To test for the presence of oxygen, the DMDO reaction with complex **1-NCAr**$^+$ was performed in an enclosed, degassed vessel. All reagents were carefully degassed, and gas samples of the reaction headspace were analyzed by GC. Traditional oxygen probes (Clark electrodes, fluorescent probes) were not compatible with acetone solutions. The reaction was scaled up and the ratio of DMDO to iridium was increased from 1:1 to 6:1, to generate detectable levels of oxygen. When 6 equiv of DMDO were added to 1 equiv of **1-NCAr**$^+$ in acetone at −40 °C, oxygen evolution started, and profiles of percent yield of oxygen versus time for multiple reactions are shown in Figure 3. To the best of our knowledge, only one example of oxygen production from DMDO decay has been reported, and that was when DMDO was treated with deprotonated peroxy acids.[32] A background reaction in the absence of iridium was also monitored, and only trace amounts of oxygen were detected

dx.doi.org/10.1021/ic4016405 | Inorg. Chem. 2013, 52, 11351−11360

Scheme 6. Styrene Oxidation Reactions Using PhIO as a Sacrificial Oxidant

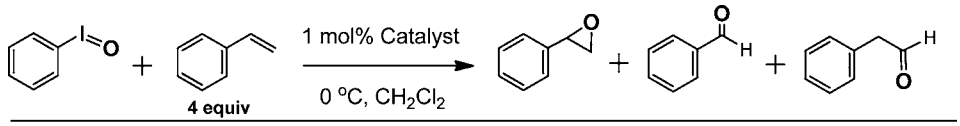

Experiment (Reference)	Catalyst	Conversion of PhIO	Yield (based on reacted PhIO) Styrene Oxide	Benzaldehyde	2-phenyl-acetaldehyde	Total
a (25)	**1-OH$_2^+$**	100% (12 hrs)	40%	6%	0%	46%
b (This Work)	**1-OH$_2^+$**	69% (24 hrs)	0%	11%	11%	22%
c (This Work)	**1-Sty$^+$**	64% (24 hrs)	0%	6%	6%	12%

when compared to reactions with **1-NCAr**$^+$ (Supporting Information, Figure S6). The GC was calibrated using known samples, and oxygen levels measured in the background reaction were subtracted from the runs with catalyst to determine overall yield.

Oxygen was clearly produced, but each profile of percent yield of oxygen over time showed dramatically different behavior. The erratic data were confusing, so two reactions were run side-by-side (Figure 3, samples C and D). Inconsistent results were observed yet again. Some traces showed nearly linear behavior, while other reactions exhibited marked induction periods. Yields varied dramatically (50%–94%, based on DMDO). It became clear that highly variable processes were occurring during the reactions. The induction periods observed for samples A and D also raised concerns that oxidative degradation or particle formation from **1-NCAr**$^+$ had to occur before oxygen evolution started. The irregular behavior could not be attributed to the presence of oxone (a reagent in the synthesis of DMDO),[30] as DMDO was distilled away from the reaction mixture. Note that carbon dioxide, a decomposition product of $[Ir(phpy)_2(OH_2)]^+$ in the presence of excess CAN, was not observed in the GC analysis.[1]

When the reaction with a 6:1 ratio of DMDO to **1-NCAr**$^+$ was run in deuterated solvent (acetone-d_6) and monitored by NMR spectroscopy at −40 °C, the Cp* methyl signals and the phpy resonances of **1-NCAr**$^+$ disappeared over 2 h at the same time as the nitrile ligand was displaced. No minor species or decomposition products such as glycolic, formic, or acetic acids were observed in the NMR spectra, unlike the results of Grotjahn[13] and Macchioni[14,15] in CAN oxidations of Ir(Cp*) complexes. Meanwhile, the DMDO slowly disappeared over 5 h (Figure 4). The results from the NMR experiment were reproducible. The NMR data and concentration versus time profiles suggest either ligand oxidation and particle formation or generation of a paramagnetic iridium species (perhaps akin to the resting state of homogeneous catalysts oxidized by sodium periodate).[18,33] It was difficult, therefore, to definitively identify the species responsible for oxygen evolution. In view of these results a homogeneous Ir(III)/Ir(V) mechanism, as we originally postulated, seems unlikely. We believe that oxygen evolution cannot be unambiguously assigned to molecular Ir(V)oxo species in water oxidation catalysis. As this study with DMDO and other oxidations with CAN demonstrate,[11−15] harsh oxidants can lead to complex reactions and variable rates of oxygen evolution, results which are not compatible with a well-behaved molecular catalyst.

Oxidation with Iodosobenzene (PhIO). Generation of $[Ir^V(Cp^*)(phpy)O]^+$ has also been invoked to explain olefin oxidations.[4,9] For example, a styrene epoxidation catalyzed by **1-OH$_2^+$** in the presence of the sacrificial oxidant PhIO gave oxidation products in 46% yield (Scheme 6, experiment a).[25] The reactive species was proposed to be $[Ir^V(Cp^*)(phpy)O]^+$. The reaction, however, took 12 h, and the mixture changed from yellow to green upon addition of oxidant, perhaps indicating formation of a heterogeneous component.[13,16] In addition, acetoxylation of a Cp* methyl group was observed in a related oxidation of Ir(Cp*)(phpy)Me with $PhI(OAc)_2$.[34] Our goal was to investigate the nature of the iridium catalyst in the epoxidation reaction in greater detail.

The epoxidation reaction with **1-OH$_2^+$** was carefully repeated in our lab, but our results differ from literature reports. Only 69% of the PhIO had reacted after 24 h (Scheme 6, experiment b), while the previously reported reaction was complete after 12 h. Of the PhIO consumed, only 22% of the oxidative equivalents yielded oxidized styrene derivatives, corresponding to a turnover number of 15. Nearly 55 oxidative equivalents (relative to iridium) were unaccounted for. The products of styrene oxidation were 2-phenylacetaldehyde and benzaldehyde, in approximately equimolar ratios. No styrene epoxide was observed, which was the major product reported in the literature; however, the phenylacetaldehyde product likely forms via acid-catalyzed rearrangement of styrene epoxide.[35,36] Although the mechanism for formation of benzaldehyde is not understood, it has also been observed as a product in styrene epoxidation reactions catalyzed by manganese porphyrins.[37] Iridium had to be present for styrene oxidation to occur.

After filtering off unreacted PhIO, the filtrate was loaded onto a short silica gel plug. All of the organic compounds were eluted with dichloromethane, and then the inorganic species were eluted with acetone. After removing the eluent of the metal-containing fractions in vacuo, the solids were dissolved in dichloromethane-d_2 and analyzed by NMR spectroscopy. The spectrum showed extensive ligand degradation, and **1-OH$_2^+$** was not observed (Supporting Information, Figure S7). A host of low intensity, sharp resonances (presumably oxidized ligand fragments) surrounded broad resonances at 7.3 ppm, 4.1 ppm, and 1.8 ppm. Complicated NMR spectra have also been observed by Grotjahn in CAN oxidations of Ir(Cp*) catalysts.[13] Additionally, acetic acid, observed multiple times as a decomposition product of Ir(Cp*) catalysts in CAN oxidations, was detected in an NMR spectrum of the crude reaction mixture.[12−15] The majority of oxidative equivalents in the epoxidation reaction likely participate in oxidation of the ligands, and the active iridium species could not be easily identified.

In the absence of oxidant, styrene readily displaced the aqua ligand of **1-OH$_2^+$** to form **1-Sty**$^+$. Complex **1-Sty**$^+$ is a potential intermediate before the onset of catalyst decomposition. The epoxidation experiment was repeated with independently synthesized **1-Sty**$^+$, and similar results were obtained. After 24

dx.doi.org/10.1021/ic4016405 | Inorg. Chem. 2013, 52, 11351−11360

Scheme 7. Proposed Electrochemical Oxidation of 1-OH_2^+ to Generate an $[Ir^V(Cp^*)(phpy)O]^+$ Intermediate by Sequential PCET Steps in Aqueous Solution

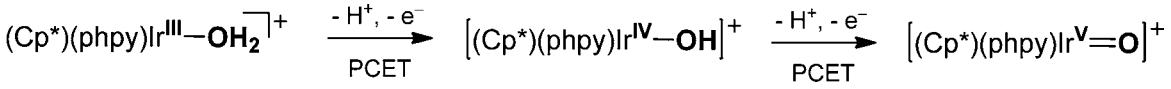

h, 64% of the PhIO reagent had been consumed (Scheme 6, experiment c). Equimolar amounts of 2-phenylacetaldehyde and benzaldehyde were observed once again, but only in a total yield of 12% (based on PhIO consumed). Acetic acid was also identified in the NMR spectrum of the crude reaction materials. Isolation of the iridium species was accomplished again using a silica gel plug, and NMR spectroscopy likewise revealed significant ligand decomposition, along with the three characteristic broad peaks (Supporting Information, Figure S8). One of the minor species in both spectra included an α-olefin pattern (presumably a bound styrene), but this was distinct from **1-Sty**$^+$. It is clear that the iridium complexes undergo oxidative degradation to unidentified species in the presence of excess PhIO. The exact nature of the precatalyst has little influence on the reaction, which would be expected if there is significant ligand degradation. It is possible that an Ir(V)oxo complex is the iridium species responsible for styrene oxidation, but degradation of the ligand framework complicates any assignment. Oxidations with PhIO, like oxidations with CAN, lead to degradation of Ir(Cp*)(phpy) complexes and generation of acetic acid.

Electrochemical Oxidation. When it became apparent that OAT would not allow a definitive spectroscopic glimpse of $[Ir^V(Cp^*)(phpy)O]^+$ in situ, attempts were made to detect an Ir(V)oxo intermediate with electrochemical methods. Electrochemical oxidation of **1-OH_2^+** in an aqueous environment (Ag/AgCl reference electrode (3 M NaCl; 0.197 V vs NHE), Pt-wire counter electrode) could yield the Ir(V)oxo complex via sequential PCET events (Scheme 7). Complex **1-OH_2^+** and the two products of PCET processes were good targets to study because they were originally proposed as intermediates for homogeneous water oxidation using the precatalyst **3**.[4] A PCET process is easily identified by observable pH dependent redox processes that follow Nernstian behavior.[38,39]

Solutions of **[1-OH_2][B(Ar^F)$_4$]** in water/ethylene carbonate (2:1 v:v) with added 0.1 M phosphate buffer and 0.5 M supporting electrolyte ($NaClO_4$) were prepared for electrochemistry. Ethylene carbonate aids solubility of **[1-OH_2][B(Ar^F)$_4$]** in water and is noncoordinating. Cyclic voltammograms (CVs) using a freshly polished glassy carbon working electrode at different pHs and scan rates, however, were featureless and poorly defined. For example, a freshly prepared 0.73 mM solution of **[1-OH_2][B(Ar^F)$_4$]** in a water/ethylene carbonate mixture at pH = 7.0 (0.1 M phosphate buffer, 0.5 M $NaClO_4$) passed a steadily increasing current at potentials higher than 0.8 V (vs NHE) at a scan rate of 100 mV s^{-1} (Figure 5a). No reversible or clean oxidations were observed. CVs of the water/ethylene carbonate solvent (2:1 v:v, pH = 7.0, 0.1 M phosphate buffer, 0.5 M $NaClO_4$) showed that background oxidation of the solvent was not significant until potentials exceeded 1.5 V.[40] Differential pulse voltammograms (DPV) also did not show well-defined oxidations of the complex, although there were three to four overlapping events between 0.6 and 1.4 V (Figure 5b). Acidic solutions (pH = 2.4, 0.1 M phosphate buffer, 0.5 M $NaClO_4$) also did not yield useful electrochemical data (Supporting Information). Since

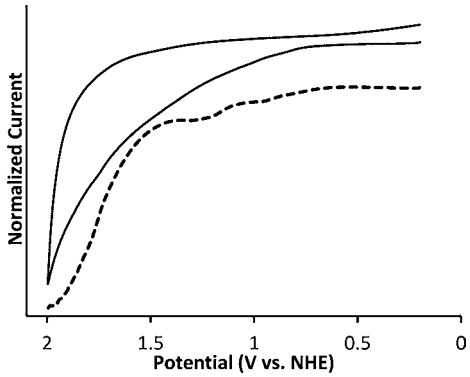

Figure 5. (a) Cyclic voltammogram of **[1-OH_2][B(Ar^F)$_4$]** in water/ethylene carbonate (2:1 v:v) at pH 7.0 (0.1 M phosphate buffer, 0.5 M $NaClO_4$) at 100 mV s^{-1} with a glassy carbon working electrode (0.07 cm^2, solid line). (b) Differential pulse voltammogram of **[1-OH_2][B(Ar^F)$_4$]** (dashed line, offset) at 23 ± 3 °C.

there were no clear, reversible redox events at either pH, it was not possible to identify PCET processes. Electrochemistry of the precatalyst **3** in water/ethylene carbonate solutions at pH = 7.0 also did not reveal reversible waves and suggested catalyst decomposition (Supporting Information). All electrochemical data pointed to chemical alteration of the catalyst when oxidized at high potentials, an outcome which is in agreement with the chemical oxidants studied. The chemical and electrochemical oxidations in this work demonstrate that catalyst decomposition is facile under harshly oxidizing conditions.

Isolation of a Silver-Bridged Dinuclear Iridium Species. A single, unexpected, product was isolated from an attempted one-pot synthesis of Ir(Cp*)(phpy)(OH).[41] Complex **1-OH_2^+** was formed according to the literature procedure by mixing **3** and 1.1 equiv of AgOTf in methanol/water (30:1.3 v:v).[25] After stirring for 1 h, 1.4 equiv of aqueous NaOH were added *prior to filtering*. A silver-bridged dinuclear iridium hydride species, [{Ir(Cp*)(phpy)H}$_2$Ag][OTf], was isolated (**2**, Scheme 8). The expected deprotonated product, Ir(Cp*)(phpy)(OH), either formed transiently or did not form at all. The structure of **2** was unequivocally established via X-ray diffraction studies on a suitable crystal (Figure 6),[42] and the terminal hydrides were confirmed by NMR spectroscopy. The dinuclear complex is nearly centrosymmetric, which made refinement using least-squares difficult. Instead, gradient

Scheme 8. Synthesis of 2[a]

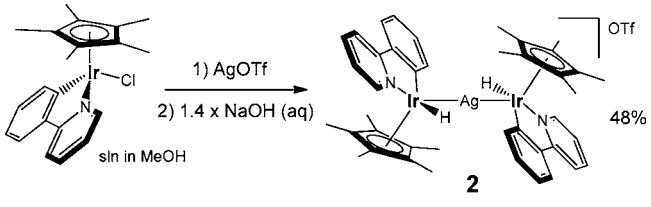

[a]Sodium hydroxide must be added prior to filtering off AgCl.

dx.doi.org/10.1021/ic4016405 | Inorg. Chem. 2013, 52, 11351−11360

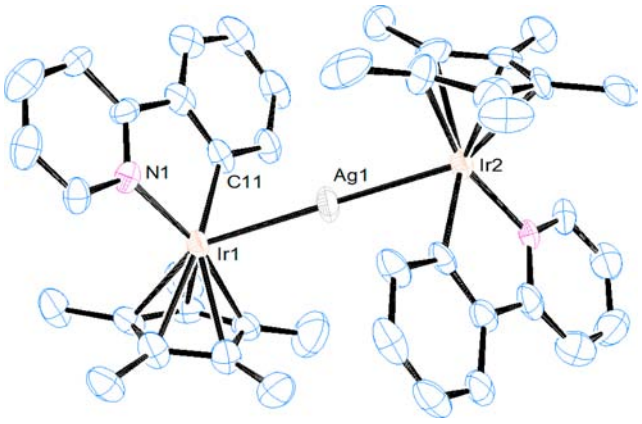

Figure 6. ORTEP drawing of **2** with partial numbering scheme. Ellipsoids are drawn at the 50% probability level. The anion and the hydrogen atoms are omitted for clarity. The terminal hydrides were observed by NMR spectroscopy, but were not located during refinement of the crystallographic data. Selected bond lengths (Å) and bond angles (deg): Ir_1–Ag_1 2.7176(6), Ir_2–Ag_1 2.7150(6), Ir_1–C_{11} 2.055(8), Ir_1–N_1 2.031(7), Ag_1–Ir_1–C_{11} 71.35(19), N_1–Ir_1–Ag_1 108.23(18), C_{11}–Ir_1–N_1 77.9(3).

refinement was used. Silver-bridged iridium complexes are known, and the Ir–Ag bond lengths of 2.718 Å and 2.715 Å for **2** are as expected for such complexes when hydrides are present.[43−46] The Ir–Ag–Ir bridge is essentially linear (bond angle of 179.35 degrees), and each Ir(Cp*)(phpy)(H)(Ag) fragment resembles a four-legged piano stool. If one considers each iridium to form a dative bond to Ag^+, the iridium cores would formally be seven-coordinate iridium(III), donating a metal electron pair to silver. This provides evidence that the Ir(Cp*)(phpy) framework is electron-donating. Oxidation products seem to be unstable, as demonstrated in the chemical and electrochemical oxidations reported, but stable products with electron-donating Ir(III) centers, such as **2**, may be isolated. Hydrides are known to stabilize higher oxidation states of iridium.[47,48]

The formation of **2** from **1-OH$_2$**$^+$ upon addition of base was investigated, as the sources of the hydrides and the silver bridge were not readily apparent. It was postulated that the hydride ligands were formed via hydride elimination from sodium methoxide, generating formaldehyde. Hydroxide and methoxide exist in equilibrium because of their similar pK_a's. The ratio of methoxide to hydroxide was calculated to be 16:1 for a mixture of 30 mL of methanol (pK_a = 15.5) and 1.3 mL of water (pK_a = 15.7), the conditions of the reaction. The addition of NaOH to methanol, therefore, predominantly yielded NaOMe.

To test the hypothesis that methoxide was acting as the hydride source, 5 mg of **1-OH$_2$**$^+$ (7.7 μmol) was treated with approximately 1 mg of NaOMe (19 μmol) in 0.5 mL of methanol-d_4. The added base exchanged rapidly with methanol-d_4, leading to formation of sodium methoxide-d_3. Clean conversion to a new metal species was observed by NMR spectroscopy, and the product was identified as Ir(Cp*)(phpy)D.[24] The formation of the deuteride complex from **1-OH$_2$**$^+$ and $NaOCD_3$ lent support to the hypothesis that methoxide was the source of the terminal hydrides of **2**. Whether the deuteride was transferred via an outer sphere or inner sphere mechanism is unclear. In either case, the aqua ligand appeared to be innocent, acting strictly as a labile ligand. Formaldehyde-d_2 generated as a byproduct would not be observed in the NMR experiment. When the reaction was performed on a preparative scale in methanol (CH_3OH), the isolated product was the same as the product of the NMR experiment, and it included a singlet for the hydride at −15.0 ppm.[24]

The source of Ag^+ in **2** could not be excess AgOTf, as the 1.1 equiv of AgOTf converted to AgCl in the presence of Ir(Cp*)(phpy)Cl (**3**). This suggested instead that the silver source was silver chloride. To test the reactivity of silver chloride, 3.5 mg of the isolated monomeric Ir(Cp*)(phpy)H complex (7.2 μmol) was mixed with 7 mg of AgCl (48 μmol) in 0.5 mL of methanol-d_4. NMR spectroscopy revealed clean formation of the dinuclear iridium complex [{Ir(Cp*)(phpy)-H}$_2$Ag][Cl] (**2-Cl**) after 12 h. Notably, the hydride did not exchange with deuterated solvent. The hydride resonance shifted upfield to −11.7 ppm and appeared as a doublet, with a J_{H-Ag} coupling constant of 77 Hz. Silver has two isotopes with nuclear spins of 1/2 with nearly identical gyromagnetic ratios. The spectrum was not sufficiently resolved to observe the two nearly equal coupling constants expected for the two silver isotopes. Formation of **2-Cl** verified that Ir(Cp*)(phpy)H extracts Ag^+ from AgCl. Synthesis of **2-Cl**, therefore, is proposed to occur via hydride elimination from methoxide to form Ir(Cp*)(phpy)H, followed by Ag^+ abstraction from AgCl, as shown in Scheme 9. Although silver chloride is not often

Scheme 9. Proposed Mechanism for the Formation of 2-Cl, Starting from 1-OH$_2$ $^{+a}$

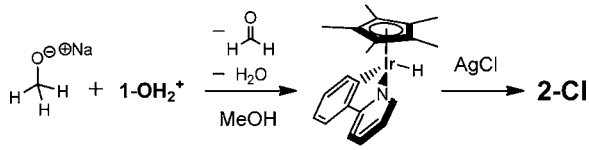

[a]The individual steps were completed in two separate NMR experiments.

considered a Ag^+ source, it has found increasing use as a reagent in the synthesis of silver complexes with coordinated *N*-heterocyclic carbenes, which are useful transmetallating reagents.[49,50] Other silver sources, such as AgOTf and $AgSbF_6$, can be used in place of silver chloride.

In solution, the two Ir(Cp*)(phpy)H units of dinuclear **2** were magnetically equivalent, so only one set of resonances for the Cp* groups and the terminal hydrides were observed. The aromatic region, however, showed sharp and broad resonances. Variable temperature ^{1}H NMR spectroscopy (Supporting Information) revealed dynamic processes due to interconversion of diastereomers of **2**. At −60 °C, two diastereomers were observed in approximately a 2:1 ratio. Two distinct hydride signals were also seen as doublets between −11.5 and −12.0 ppm, with differing J_{H-Ag} coupling constants of 87 and 90 Hz for the two diastereomers.[51] The two distinct coupling constants expected for the two isotopes of silver could not be resolved for any hydride resonance at any temperature. The chemical shifts of the hydride signals for the isomeric complexes were temperature dependent; the two doublets moved together and overlapped to form a pseudotriplet at −20 °C.

Few changes occurred in the alkyl and aromatic regions of the ^{1}H NMR spectrum between −60 °C and −20 °C. The two Cp* peaks stayed well-resolved and sharp. There were 10 separate resonances in the aromatic region (one would expect

dx.doi.org/10.1021/ic4016405 | Inorg. Chem. 2013, 52, 11351−11360

16 independent resonances for two diastereomers), but multiple peaks were clearly overlapping. Interconversion on an NMR time scale between the two diastereomers was visible at 0 °C. The Cp* and hydride resonances broadened and merged, but the hydrides maintained their coupling to silver (both J_{H-Ag} values were 85 Hz), indicating an intramolecular conversion between the diastereomers. Analysis of line broadening on the Cp* signal of the major diastereomer at 0 °C allowed a rate constant for conversion of the major to the minor isomer of 29 s^{-1} ($\Delta G^{\ddagger}$ = ca. 14 kcal/mol) to be extracted. In the aromatic region, four signals were sharp relative to at least six broad signals. The sharp signals were identified as pyridine protons, and the position of these peaks did not change upon warming or cooling. The pyridine resonances, therefore, had almost identical chemical shifts in the two diastereomers and did not noticeably broaden at the onset of interconversion. Six of the eight broad resonances expected for exchanging phenyl protons for the two diastereomers were observed.

The Cp* peaks and the hydride resonances coalesced at 30 °C, and the hydrides were still coupled to silver (J_{H-Ag} = 77 Hz). The four sharp pyridine proton resonances in the aromatic region were complemented by four broad phenyl proton resonances, and the phenyl proton resonances continued to sharpen as the temperature was raised to 50 °C. At this point, the hydride coupling to silver was lost and the resonance for the hydrides coalesced into a singlet, indicating rapid dissociation/reassociation of an Ir(Cp*)(phpy)H fragment. The phenyl protons could not be fully resolved at higher temperatures because the molecule was thermally unstable.

CONCLUSIONS

Oxidation to form observable high-valent iridium species is challenging, especially when the target is an Ir(V)oxo species. Oxidation using OAT reagents provided some encouraging initial results, as oxidation of **1-NCAr**$^+$ with DMDO yielded dioxygen. In addition, some oxidized styrene products were observed in the presence of **1-OH$_2$**$^+$ and PhIO. Further investigation, however, revealed extensive ligand oxidation or suggested a heterogeneous component, and molecular Ir(V)oxo complexes could not be definitively implicated in either system. Acetic acid, a decomposition product observed for oxidation with CAN, was also identified in oxidations with PhIO. These results demonstrate that oxidation to high-valent iridium species with retention of ligand identity cannot be assumed. These conclusions are strengthened by the aqueous electrochemistry of **1-OH$_2$**$^+$, which was unstable when oxidized electrochemically. While all of these results reflect the instability of high-valent iridium species, it was found that the Cp* and phpy ligands supported the formation of **2**, a stable dinuclear iridium species with an expanded coordination sphere at iridium. Complex **2** presumably formed from the reaction of Ir(Cp*)(phpy)H and AgCl. The reactivity observed with silver chloride is a rare example of Ag^+ extraction from AgCl.

EXPERIMENTAL SECTION

Materials and Methods. All reactions were performed under an atmosphere of dry argon using standard Schlenk and drybox techniques, unless noted otherwise. Argon was purified by passage through columns of BASF R3-11 catalyst and 4 Å molecular sieves. Methylene chloride, hexanes, and pentane were purified under an argon atmosphere and passed through a column packed with activated alumina. All other chemicals were used as received without further purification. ^{1}H and ^{13}C NMR spectra were recorded on Bruker DRX400, AVANCE400, and AMX300 spectrometers. ^{1}H NMR and ^{13}C NMR chemical shifts were referenced to residual ^{1}H and ^{13}C signals of the deuterated solvents. X-ray diffraction studies were conducted on a Bruker-AXS SMART APEX-II diffractometer. Suitable crystals were selected and mounted using a paratone oil on a MiteGen mylar tip. Elemental analyses were performed by Robertson Microlit Laboratories of Madison, NJ.

Electrochemistry. Electrochemical measurements were conducted on a CH Instruments 660D potentiostat with a glassy carbon working electrode (0.07 cm^2), Pt-wire counter electrode, and Ag/AgCl reference (saturated NaCl, 0.197 V vs NHE). $E_{1/2}$ values were obtained from the peak currents in differential pulse voltammograms and are reported vs the normal hydrogen electrode (NHE). The glassy carbon working electrode was polished on alumina paste, rinsed with water, and dried before each use.

Synthesis of Ir(Cp*)(phpy)Cl (3). The compound was prepared as reported.[23]

Synthesis of [Ir(Cp*)(phpy)(3,5-bis(trifluoromethyl)-benzonitrile)][B(Ar^F)$_4$] (1-NCAr$^+$). A 100 mL Schlenk flask was charged with 720 mg of Na[B(Ar^F)$_4$] (0.81 mmol), 150 μL of 3,5-bis-(trifluoromethyl)benzonitrile (0.89 mmol), and 20 mL of dichloromethane. A 360 mg portion of Ir(Cp*)(phpy)Cl (0.70 mmol) was added, and the solution was stirred for 24 h at room temperature. The reaction mixture was filtered, and the solvent of the filtrate was reduced to a minimal volume. The concentrated solution was slowly added to rapidly stirring pentanes chilled to −78 °C. The mixture was filtered, and the bright yellow solid was heated at 50 °C overnight under vacuum, yielding 920 mg product (82%). Anal. Calcd. (found) for $C_{62}H_{38}N_2BF_{30}Ir$: C, 47.01 (47.10); H, 2.42 (2.70); N, 1.77 (1.78). ^{1}H NMR (600 MHz, CD_2Cl_2) δ 8.65 (d, J = 5.4, 1H), 8.15 (s, 1H), 7.96 (d, J = 8.4, 1H), 7.88 (t, J = 7.8, 1H), 7.83 (s, 2H), 7.78 (t, J = 8.4, 2H), 7.72 (s, 8H), 7.55 (s, 4H), 7.34 (t, J = 7.2, 1H), 7.23−7.27 (m, 2H), 1.72 (s, 15H). ^{13}C{^{1}H} NMR (150 MHz, CD_2Cl_2) δ 167.7, 161.7 (1:1:1:1 quartet, J_{C-B} = 50), 155.1, 151.7, 144.6, 139.7, 135.6, 134.8, 133.5, 133.3, 132.2, 128.8 (q, 2 bond J_{C-F} = 29), 128.4, 124.6 (q, 1 bond J_{C-F} = 271), 124.9, 124.6, 123.9, 121.9 (q, 1 bond J_{C-F} = 269), 120.3, 117.5, 116.6, 112.2, 92.7, 8.7.

Synthesis of [Ir(Cp*)(phpy)(styrene)][B(Ar^F)$_4$] (1-Sty$^+$). To a solution of 200 mg of Ir(Cp*)(phpy)Cl (0.39 mmol) in 30 mL of dichloromethane were added 400 mg of Na[B(Ar^F)$_4$] (0.45 mmol, 1.2 equiv) and 90 μL of styrene (0.79 mmol, 2 equiv). The mixture was filtered after stirring for 2 h, and the filtrate was reduced to minimal volume, cooled to −78 °C, and filtered again. The concentrated solution was added dropwise to 40 mL of rapidly stirring hexanes cooled to −40 °C. The precipitate was collected via filtration and dried, yielding 266 mg of pale yellow solid (47%). The ^{1}H NMR spectrum and ^{13}C NMR spectrum revealed the presence of a major and minor isomer (~4:1 ratio). Multiple resonances overlapped in the ^{1}H NMR spectrum. Anal. Calcd. (found) for $C_{61}H_{43}NBF_{24}Ir$: C, 50.56 (50.33); H, 2.99 (2.78); N, 0.97 (0.93). ^{1}H NMR (500 MHz, CD_2Cl_2) δ (Major isomer) 7.72 (s, 9H), 7.63 (d, J = 10.0, 2H), 7.56 (s, 4H), 7.54 (t, J = 10.5, 1H), 7.40 (m, 2H) 7.30 (t, J = 9.5, 1H), 6.98 (t, J = 9.0, 1H), 6.84 (t, J = 9.5, 1H), 6.59 (t, J = 7.5, 1H), 4.78 (dd, J = 11.0 and 14.5, 1H), 3.61 (m, 2H), 1.57 (s, 15H); δ (Minor isomer; multiple resonances were unobserved) 8.19 (d, J = 7.0, 1H), 7.88 (t, J = 9.0, 1H), 7.13 (t, J = 9.5, 1H), 7.04 (t, J = 9.5, 1H), 6.95 (t, J = 10.5, 1H), 6.28 (t, J = 9.0, 2H), 4.51 (dd, J = 10.0 and 15, 1H), 3.77 (dd, J = 11.0 and 1.5, 1H), 3.57 (partially overlapping, 1H), 1.57 (shoulder on major isomer, 15H). ^{13}C{^{1}H} NMR (125 MHz, CD_2Cl_2) δ (Major isomer, one carbon merged to others) 166.0, 162.1 (1:1:1:1 quartet, J_{C-B} = 51), 153.2, 151.8, 143.8, 139.1, 136.7, 135.5, 135.2, 132.0, 129.2 (q, 2 bond J_{C-F} = 31), 129.0, 128.5, 125.7, 125.5, 125.0 (q, 1 bond J_{C-F} = 270), 123.5, 119.8, 117.9 (pseudo t, J = 15), 100.5, 70.6, 46.6, 8.2; δ (Minor isomer, one carbon merged to others) 167.6, 162.1 (1:1:1:1 quartet, J_{C-B} = 51), 156.8, 152.8, 142.9, 140.3, 135.9, 135.7, 135.2, 129.2 (q, 2 bond J_{C-F} = 31), 128.2, 128.0, 126.4, 125.6, 125.0 (q, 1 bond J_{C-F} = 270), 124.9, 124.3, 120.6, 117.9 (pseudo t, J = 15), 100.3, 71.2, 49.0, 8.6.

dx.doi.org/10.1021/ic4016405 | Inorg. Chem. 2013, 52, 11351−11360

Synthesis of [Ir(Cp*)(phpy)(OH_2)][OTf] (1-OH_2^+). The compound was prepared as reported.[25] Crystals suitable for X-ray diffraction were obtained by layering pentane on top of a concentrated solution in dichloromethane.

Synthesis of [Ir(Cp*)(phpy)(OH_2)][$B(Ar^F)_4$] ([1-OH_2][$B(Ar^F)_4$]). A 100 mL Schlenk flask was charged with 376 mg of [Ir(Cp*)(phpy)(OH_2)][OTf] (0.58 mmol), 525 mg of Na[$B(Ar^F)_4$] (0.59 mmol), and 20 mL of dichloromethane. After stirring for 30 min, the mixture was filtered, and the solvent of the filtrate was reduced to a minimal volume. The solution was slowly added to 30 mL of rapidly stirring pentanes at −40 °C. The precipitate was isolated by filtration and heated under vacuum at 50 °C overnight, yielding 546 mg of a deep red solid (69%). Anal. Calcd. (found) for $C_{53}H_{37}NBF_{24}IrO$: C, 46.71 (46.98); H, 2.74 (2.66); N, 1.03 (1.04). ^{1}H NMR (500 MHz, CD_3OD) δ 8.94 (d, J = 5.5, 1H), 8.09 (d, J = 8.0, 1H), 8.02 (d, J = 7.5, 1H), 7.97 (t, J = 7.5, 1H), 7.83 (d, J = 7.5, 1H), 7.59 (s, 12H), 7.40 (t, J = 6.0, 1H), 7.28 (t, J = 7.5, 1H), 7.16 (t, J = 7.5, 1H), 1.65 (s, 15H). $^{13}C\{^1H\}$ NMR (125 MHz, CD_3OD) δ 169.3, 162.7 (1:1:1:1 quartet, J_{C-B} = 49), 162.3, 153.3, 147.5, 141.0, 136.9, 135.8, 132.6, 130.4 (q, 2 bond J_{C-F} = 31), 125.7 (q, 1 bond J_{C-F} = 270), 125.5, 125.4, 125.3, 120.8, 118.7, 89.6, 9.1.

Synthesis of [{Ir(Cp*)(phpy)H}$_2$Ag][OTf] (2). A 100 mL Schlenk flask was charged with 30 mL of methanol, 1.3 mL of water, 300 mg of Ir(Cp*)(phpy)Cl (0.58 mmol), and 155 mg of AgOTf (0.60 mmol). After stirring for 1 h in the dark, 160 μL of 5 M aqueous NaOH (0.80 mmol, 1.4 equiv) was added, and the solution immediately turned red. After stirring for 20 min, the color had changed to a pale yellow-green. The reaction was stirred for five additional hours and then filtered. The solvent of the filtrate was removed under reduced pressure, and the solid was redissolved in minimal methanol. Water was slowly added to the solution to precipitate the product, which was isolated by filtration. The solid was then redissolved in minimal, hot isopropanol, filtered, and slowly added to rapidly stirring hexanes chilled to −40 °C. After storing overnight at −30 °C, the mixture was filtered, and 169 mg of a yellow-green solid was isolated after drying under high vacuum for 4 h (48%). Crystals suitable for X-ray diffraction were obtained by layering hexanes on top of a concentrated solution in 2-propanol. Anal. Calcd. (found) for $C_{43}H_{48}N_2AgF_3Ir_2O_3S$: C, 42.26 (42.33); H, 3.96 (3.86); N, 2.29 (2.30). ^{1}H NMR (500 MHz, CD_3OD) δ 8.72 (d, J = 5.5, 2H), 7.92 (s, 2H), 7.77 (t, J = 7.5, 2H), 7.67 (s, 2H), 7.42 (d, J = 7.5, 2H), 7.12 (t, J = 6.5, 2H), 6.90 (s, 2H), 6.63 (s, 1−2H), 1.74 (s, 30H), −11.70 (d, J_{H-Ag} = 77 Hz, 2H).

Synthesis of Ir(Cp*)(phpy)H. The compound can be prepared as reported.[24] An additional synthesis is given here. A solution of 100 mg of Ir(Cp*)(phpy)Cl (0.19 mmol) and 85 mg of NaOMe (1.57 mmol, 8 equiv) in 20 mL of methanol was stirred for 7 h, at which point the solvent was removed. Twenty-five milliliters of water were added, and the mixture was sonicated for 20 min. The mixture was filtered, and the pale orange solid was dried in air for 3 h, yielding 48 mg solid (49%). The hydride exchanged for chloride in chlorinated solvents. Anal. Calcd. (found) for $C_{21}H_{24}NIr{\cdot}H_2O$: C, 50.38 (50.31); H, 5.23 (4.93); N, 2.80 (2.61).

NMR-Tube Reaction of DMDO and 1-NCAr$^+$, 1:1. An acetone solution of DMDO (70 μL, 0.057 M, 4.0 μmol) was added slowly to an NMR tube chilled to −80 °C and containing a solution of **1-NCAr**$^+$ (6.0 mg, 3.8 μmol) in 0.5 mL of acetone-d_6. The reaction was transported at −80 °C to an NMR probe cooled to the same temperature. The onset of the reaction occurred upon warming to −50 °C, and the reaction progress was monitored by NMR spectroscopy. After the DMDO had reacted, at least 90% of the original **1-NCAr**$^+$ compound was intact, and no new iridium species was observed.

Reactions of DMDO and 1-NCAr$^+$, 6:1, Monitored by GC. Conditions of a representative reaction are described. A 10 mL round-bottom flask was charged with 11.9 mg of **1-NCAr**$^+$ (7.5 μmol) and 1.6 mL of acetone, and then tightly capped with a serrated silicone rubber septum. The solution was cooled to −40 °C and sparged with nitrogen for 5 minutes. A 0.5 mL portion of a degassed acetone solution of DMDO (0.091 M, 45.5 μmol, 6.1 equiv) was added slowly via syringe, and the reaction was gently stirred at −40 °C. Samples of the reaction headspace were taken periodically with a gastight syringe and analyzed by GC to determine percent yield of dioxygen.

NMR-Tube Reaction of DMDO and 1-NCAr$^+$, 6:1. A 15% acetone: 85% acetone-d_6 (v:v) solution of DMDO and DMDO-d_6 (15:85 ratio, 0.123 M, 65 μL, 8 μmol) was added slowly to an NMR tube chilled to −80 °C and containing a solution of **1-NCAr**$^+$ (2.0 mg, 1.3 μmol) in 0.5 mL of acetone-d_6. The reaction was monitored by NMR spectroscopy at −40 °C. The resonances of **1-NCAr**$^+$ disappeared over 2 h, and the nitrile ligand was displaced. No new iridium species was observed, and the DMDO continued to react over 5 h.

Styrene Oxidation with PhIO and 1-OH_2^+. A solution of 7.0 mg of **1-OH_2^+** (0.01 mmol) in 2.5 mL of dichloromethane was slowly added to a mixture of 220 mg of PhIO (1.0 mmol) and 460 μL of styrene (4.0 mmol) in 2.5 mL of dichloromethane cooled to 0 °C. The reaction was stirred for 24 h at 0 °C, at which point the insoluble PhIO was removed from the reaction mixture by filtration. A drop of the filtrate was added to dichloromethane-d_2 and analyzed by ^{1}H NMR spectroscopy to identify reaction products and determine yields. The filtrate was then concentrated under reduced pressure and loaded onto a short silica gel plug (10 cm). After the organic compounds were eluted with dichloromethane, acetone was used as the eluent to retrieve the inorganic species. The solvent was removed under reduced pressure, and the solids were redissolved in dichloromethane-d_2 and analyzed by NMR spectroscopy.

Styrene Oxidation with PhIO and 1-Sty$^+$. The procedure for styrene epoxidation with **1-OH_2^+** was followed, except that 15.3 mg of **1-Sty**$^+$ (0.01 mmol) was used.

■ ASSOCIATED CONTENT

Ⓢ Supporting Information

NMR spectra, including those of new compounds, the recovered metal species after epoxidation reactions, and variable temperature spectra of **2** are provided. Also included are the electrochemical studies of **3** and crystallographic information of the reported structures. This material is available free of charge via the Internet at http://pubs.acs.org.

■ AUTHOR INFORMATION

Corresponding Author

*E-mail: joetemp@unc.edu.

Present Address

†Virginia Military Institute, 403 Maury-Brooke Hall, Lexington, VA 24450.

Notes

The authors declare no competing financial interest.

■ ACKNOWLEDGMENTS

This research was primarily supported by the UNC EFRC "Center for Solar Fuels", an EFRC funded by the U.S. Department of Energy, Office of Science, Office of Basic Energy Sciences under award DE-SC0001011 supporting D.P.H. In addition C.R.T. acknowledges support from the National Science Foundation Graduate Research Fellowship Program under Grant DGE-1144081.

■ REFERENCES

(1) McDaniel, N. D.; Coughlin, F. J.; Tinker, L. L.; Bernhard, S. *J. Am. Chem. Soc.* **2008**, *130*, 210−217.

(2) Dzik, W. I.; Calvo, S. E.; Reek, J. N. H.; Lutz, M.; Ciriano, M. A.; Tejel, C.; Hetterscheid, D. G. H.; de Bruin, B. *Organometallics* **2011**, *30*, 372−374.

(3) Hetterscheid, D. G. H.; Reek, J. N. H. *Chem. Commun. (Cambridge, UK)* **2011**, *47*, 2712−2714.

(4) Blakemore, J. D.; Schley, N. D.; Balcells, D.; Hull, J. F.; Olack, G. W.; Incarvito, C. D.; Eisenstein, O.; Brudvig, G. W.; Crabtree, R. H. *J. Am. Chem. Soc.* **2010**, *132*, 16017−16029.
(5) Savini, A.; Bellachioma, G.; Ciancaleoni, G.; Zuccaccia, C.; Zuccaccia, D.; Macchioni, A. *Chem. Commun. (Cambridge, UK)* **2010**, *46*, 9218−9219.
(6) Lalrempuia, R.; McDaniel, N. D.; Müller-Bunz, H.; Bernhard, S.; Albrecht, M. *Angew. Chem., Int. Ed.* **2010**, *49*, 9765−9768.
(7) Miranda-Soto, V.; Parra-Hake, M.; Morales-Morales, D.; Toscano, R. A.; Boldt, G.; Koch, A.; Grotjahn, D. B. *Organometallics* **2005**, *24*, 5569−5575.
(8) Hull, J. F.; Balcells, D.; Blakemore, J. D.; Incarvito, C. D.; Eisenstein, O.; Brudvig, G. W.; Crabtree, R. H. *J. Am. Chem. Soc.* **2009**, *131*, 8730−8731.
(9) Zhou, M.; Schley, N. D.; Crabtree, R. H. *J. Am. Chem. Soc.* **2010**, *132*, 12550−12551.
(10) Schley, N. D.; Blakemore, J. D.; Subbaiyan, N. K.; Incarvito, C. D.; D'Souza, F. D.; Crabtree, R. H.; Brudvig, G. W. *J. Am. Chem. Soc.* **2011**, *133*, 10473−10481.
(11) Junge, H.; Marquet, N.; Kammer, A.; Denurra, S.; Bauer, M.; Wohlrab, S.; Gärtner, F.; Pohl, M.-M.; Spannenberg, A.; Gladiali, S.; Beller, M. *Chem.—Eur. J.* **2012**, *18*, 12749−12758.
(12) Wang, C.; Wang, J.-L.; Lin, W. *J. Am. Chem. Soc.* **2012**, *134*, 19895−19908.
(13) Grotjahn, D. B.; Brown, D. B.; Martin, J. K.; Marelius, D. C.; Abadjian, M.-C.; Tran, H. N.; Kalyuzhny, G.; Vecchio, K. S.; Specht, Z. G.; Cortes-Llamas, S. A.; Miranda-Soto, V.; van Niekerk, C.; Moore, C. E.; Rheingold, A. L. *J. Am. Chem. Soc.* **2011**, *133*, 19024−19027.
(14) Savini, A.; Belanzoni, P.; Bellachioma, G.; Zuccaccia, C.; Zuccaccia, D.; Macchioni, A. *Green Chem.* **2011**, *13*, 3360−3374.
(15) Zuccaccia, C.; Bellachioma, G.; Bolaño, S.; Rocchigiani, L.; Savini, A.; Macchioni, A. *Eur. J. Inorg. Chem.* **2012**, 1462−1468.
(16) Hintermair, U.; Hashmi, S. M.; Elimelech, M.; Crabtree, R. H. *J. Am. Chem. Soc.* **2012**, *134*, 9785−9795.
(17) Zhou, M.; Hintermair, U.; Hashiguchi, B. G.; Parent, A. R.; Hashmi, S. M.; Elimelech, M.; Periana, R. A.; Brudvig, G. W.; Crabtree, R. H. *Organometallics* **2013**, *32*, 957−965.
(18) Hintermair, U.; Sheehan, S. W.; Parent, A. R.; Ess, D. H.; Richens, D. T.; Vaccaro, P. H.; Brudvig, G. W.; Crabtree, R. H. *J. Am. Chem. Soc.* **2013**, *135*, 10837−10851.
(19) McGhee, W. D.; Foo, T.; Hollander, F. J.; Bergman, R. G. *J. Am. Chem. Soc.* **1988**, *110*, 8543−8545.
(20) Hay-Motherwell, R. S.; Wilkinson, G.; Hussain-Bates, B.; Hursthouse, M. B. *Polyhedron* **1993**, *12*, 2009−2012.
(21) O'Halloran, K. P.; Zhao, C.; Ando, N. S.; Schultz, A. J.; Koetzle, T. F.; Piccoli, P. M. B.; Hedman, B.; Hodgson, K. O.; Bobyr, E.; Kirk, M. L.; Knottenbelt, S.; Depperman, E. C.; Stein, B.; Anderson, T. M.; Cao, R.; Geletii, Y. V.; Hardcastle, K. I.; Musaev, D. G.; Neiwert, W. A.; Fang, X.; Morokuma, K.; Wu, S.; Kögerler, P.; Hill, C. H. *Inorg. Chem.* **2012**, *51*, 7025−7031.
(22) Poverenov, E.; Efremenko, I.; Frenkel, A.; Ben-David, Y.; Shimon, L.; Leitus, G.; Konstantinovski, L.; Martin, J. M. L.; Milstein, D. *Nature* **2008**, *455*, 1093−1096.
(23) Scheeren, C.; Maasarani, F.; Hijazi, A.; Djukic, J.-P.; Pfeffer, M. *Organometallics* **2007**, *26*, 3336−3345.
(24) Hu, Y.; Li, L.; Shaw, A. P.; Norton, J. R.; Sattler, W.; Rong, Y. *Organometallics* **2012**, *31*, 5058−5064.
(25) Sau, Y.-K.; Yi, X.-Y.; Chan, K.-W.; Lai, C.-S.; Williams, I. D.; Leung, W.-H. *J. Organomet. Chem.* **2010**, *695*, 1399−1404.
(26) Data collection was conducted using CuK$_\alpha$ radiation while the crystal of **1-OH$_2$**$^+$ was kept at −173 °C. Using Olex2,[52] the structure was solved with the XS structure solution program using direct methods and refined with the XL refinement package using least-squares minimization.[53] Summary of unit cell constants: crystal system = monoclinic; space group = $P2_1/c$; $a/b/c$ (Å) = 16.1914(4)/12.4570(3)/11.5310(3); $\alpha/\beta/\gamma$ (deg) = 90.00/107.4690(10)/90.00; Z = 4; goodness of fit on F^2 = 1.096; final R indexes (all data): R_1 = 0.0358, wR_2 = 0.0819; Largest diff. peak/hole (e Å^{-3}) = 2.13/−0.64.
(27) Ogo, S.; Makihara, N.; Kaneko, Y.; Watanabe, Y. *Organometallics* **2001**, *20*, 4903−4910.
(28) Ito, J.; Shiomi, T.; Nishiyama, H. *Adv. Synth. Catal.* **2006**, *348*, 1235−1240.
(29) Ogo, S.; Makihara, N.; Watanabe, Y. *Organometallics* **1999**, *18*, 5470−5474.
(30) Adam, W.; Chan, Y. Y.; Cremer, D.; Gauss, J.; Scheutzow, D.; Schindler, M. *J. Org. Chem.* **1987**, *52*, 2800−2803.
(31) Hull, L. A.; Budhai, L. *Tetrahedron Lett.* **1993**, *34*, 5039−5042.
(32) Curci, R.; D'Accolti, L.; Fusco, C. *Acc. Chem. Res.* **2006**, *39*, 1−9.
(33) Macchioni and coworkers were able to distinguish between molecular iridium species and nanoparticles after CAN oxidation by adding benzyl alcohol to reaction mixtures. A characteristic blue absorbance (λ = 574 nm) of the metal species faded rapidly in the presence of benzyl alcohol, suggesting a molecular metal species. The blue species was not observed in our system (both **1-NCAr**$^+$ and the reaction mixture were yellow). Savini , A.; Bucci , A.; Bellachioma , G.; Rocchigiani , L.; Zuccaccia , C.; Llobet , A.; Macchioni , A. *Eur. J. Inorg. Chem.* **2013**, Early View, http://onlinelibrary.wiley.com/doi/10.1002/ejic.201300530/abstract.
(34) Park-Gehrke, L. S.; Freudenthal, J.; Kaminsky, W.; DiPasquale, A. G.; Mayer, J. M. *Dalton Trans.* **2009**, 1972−1983.
(35) Fruetel, J. A.; Collins, J. R.; Camper, D. L.; Loew, G. H.; Ortiz de Montellano, P. R. *J. Am. Chem. Soc.* **1992**, *114*, 6987−6993.
(36) Collman, J. P.; Kodadek, T.; Brauman, J. I. *J. Am. Chem. Soc.* **1986**, *108*, 2588−2594.
(37) Liu, Y.; Zhang, H.-J.; Lu, Y.; Cai, Y.-Q.; Liu, X.-L. *Green Chem.* **2007**, *9*, 1114−1119.
(38) Liu, F.; Concepcion, J. J.; Jurss, J. W.; Cardolaccia, T.; Templeton, J. L.; Meyer, T. J. *Inorg. Chem.* **2008**, *47*, 1727−1752.
(39) Chen, Z.; Concepcion, J. J.; Hu, X.; Yang, W.; Hoertz, P. G.; Meyer, T. J. *Proc. Natl. Acad. Sci. U.S.A.* **2010**, *107*, 7225−7229.
(40) Aurbach, D. *Nonaqueous Electrochemistry*; Marcel Dekker, Inc: New York, 1999.
(41) For a viable procedure for synthesis of Ir(Cp*)(phpy)(OH), see reference 8.
(42) Data collection was conducted using CuK$_\alpha$ radiation while the crystal of **2** was kept at −173 °C. Using Olex2, the structure was solved with the olex2.solve structure solution program using charge flipping and refined with the olex2.refine refinement package using Gauss−Newton minimization.[52] Disordered solvent was modeled using the olex2 solvent masking function, which triggered an expected A-level alert in the checkCIF report. Summary of unit cell constants: crystal system = monoclinic; space group = $P2_1$; $a/b/c$ (Å) = 8.5002(2)/24.2243(5)/12.2503(2); $\alpha/\beta/\gamma$ (deg) = 90/101.345(1)/90; Z = 2; goodness of fit on F^2 = 1.048; final R indexes (all data): R_1 = 0.0362, wR_2 = 0.0947; Largest diff. peak/hole (e Å^{-3}) = 1.92/−0.81; Flack parameter = 0.46(2).
(43) Bachechi, F. *J. Organomet. Chem.* **1994**, *474*, 191−197.
(44) Feldman, J.; Calabrese, J. C. *Inorg. Chem.* **1994**, *33*, 5955−5956.
(45) Sykes, A.; Mann, K. R. *J. Am. Chem. Soc.* **1988**, *110*, 8252−8253.
(46) Einstein, F. W. B.; Jones, R. H.; Zhang, X.; Sutton, D. *Can. J. Chem.* **1989**, *67*, 1832−1836.
(47) Rhodes, L. F.; Caulton, K. G. *J. Am. Chem. Soc.* **1985**, *107*, 259−260.
(48) Jungton, A.-K.; Meltzer, A.; Präsang, C.; Braun, T.; Driess, M.; Penner, A. *Dalton Trans.* **2010**, *39*, 5436−5438.
(49) Kriechbaum, M.; Hölbling, J.; Stammler, H.-G.; List, M.; Berger, R. J. F.; Monkowius, U. *Organometallics* **2013**, *32*, 2876−2884.
(50) Zhu, S.; Liang, R.; Jiang, H. *Tetrahedron* **2012**, *68*, 7949−7955.
(51) Presumably the $J_{H\text{-}Ag}$ coupling constants showed some dependence on temperature.
(52) Dolomanov, O. V.; Bourhis, L. J.; Gildea, R. J.; Howard, J. A. K.; Puschmann, H. *J. Appl. Crystallogr.* **2009**, *42*, 339−341.
(53) SHELX: Sheldrick, G. M. *Acta Crystallogr., Sect. A.* **2008**, *64*, 112−122.